Localization and Physical Property Experiments Conducted by Opportunity at Meridiani Planum

R. E. Arvidson, *et al.*

Science **306**, 1730 (2004);
DOI: 10.1126/science.1104211

Science (print ISSN 0036-8075; online ISSN 1095-9203) is published weekly, except the last week in December, by the American Association for the Advancement of Science, 1200 New York Avenue NW, Washington, DC 20005.

Eagle crater. It may have been ejected by a large, distant impact event. Bounce rock displays an unusual surface texture dominated by polished, parallel striations, ostensibly similar to slickensides formed by differential motion under pressure in terrestrial rocks. The striated surfaces also resemble those found in shatter cones, fracture surfaces commonly found in terrestrial impact structures (*24*). MI images show lineations down to a sub-mm scale and irregular flat surfaces that may be responsible for the rock's specular reflectance (Fig. 6). The MI images further show that these features are limited to a 2- to 3-mm-thick surface that may be differentially resistant to erosion by sandblasting on Meridiani Planum. The rock interior has a rough but predominantly aphanitic texture, with some dark grains that may be phenocrysts. The rock contains mm-scale rounded clasts in exposed fractures and eroded recesses and has been fractured in a pattern that suggests compressional deformation.

References and Notes

1. S. W. Squyres *et al.*, *J. Geophys. Res.* **108**, 8062 10.1029/2003JE002121 (2003).
2. K. E. Herkenhoff *et al.*, *J. Geophys. Res.* **108**, 8065 10.1029/2003JE002076 (2003).
3. K. E. Herkenhoff *et al.*, *Science* **305**, 824 (2004).
4. A martian solar day has a mean period of 24 hours 39 min 35.244 s and is referred to as a sol to distinguish this from a ~3% shorter solar day on Earth.
5. S. W. Squyres *et al.*, *Science* **306**, 1698 (2004).
6. R. E. Arvidson *et al.*, *Science* **306**, 1730 (2004).
7. M. Madsen *et al.*, *J. Geophys. Res.* **108**, 8069, 10.1029/2002JE002029 (2003).
8. The term martian soil is used here to denote any loose, unconsolidated materials that can be distinguished from rocks, bedrock, or strongly cohesive sediments. No implication of the presence or absence of organic materials or living matter is intended.
9. Names have been assigned to geographic features by the MER team for planning and operations purposes. The names are not formally recognized by the International Astronomical Union.
10. G. Klingelhöfer *et al.*, *Science* **306**, 1740 (2004).
11. R. Rieder *et al.*, *Science* **306**, 1746 (2004). Note the abundance of salt-forming elements in soils.
12. G. M. Marion, Special Report 95-12, Cold Regions Research and Engineering Laboratory, U.S. Army Corps of Engineers (1995).
13. W. W. Dickinson, M. R. Rosen, *Geology* **31**, 199 (2003).
14. L. A. Soderblom *et al.*, *Science* **306**, 1723 (2004).
15. The ability to resolve individual grains with the MI depends on the illumination of the scene and the contrast between the grain and its surroundings. Typically, an object must subtend at least 3 pixels to be recognized in an image (about 100 μm for the MI).
16. Grain-size classifications use the Wentworth scale (*25*).
17. An example of a terrestrial eolian lag is shown in figure 6 of Greeley *et al.* (*26*).
18. J. D. Iversen, B. R. White, *Sedimentology* **29**, 111 (1982).
19. J. Bell III *et al.*, *Science* **306**, 1703 (2004).
20. P. R. Christensen *et al.*, *Science* **306**, 1733 (2004).
21. S. Gorevan *et al.*, *J. Geophys. Res.* **108**, 8068, 10.1029/2003JE002061 (2003).
22. S. W. Squyres *et al.*, *Science* **306**, 1709 (2004).
23. Although terrestrial concretions commonly contain internal structures that parallel bedding, this is by no means a ubiquitous or diagnostic feature of concretions; see (*27*).
24. R. S. Dietz, in *Shock Metamorphism of Natural Materials*, B. M. French, N. M. Short, Eds. (Mono-Books, San Francisco, CA, 1968), pp. 267–285.
25. C. K. Wentworth, *J. Geol.* **30**, 377 (1922).
26. R. Greeley *et al.*, *J. Geophys. Res.* **104**, 8573 (1999).
27. J. Sellés-Martínez, *Earth Sci. Rev.* **41**, 177 (1996).
28. The U.S. Geological Survey MER Team developed MI software and created various data products, including some of those displayed in this issue: B. Archinal, J. Barrett, K. Becker, T. Becker, D. Burr, D. Cook, D. Galuszka, T. Hare, A. Howington-Kraus, R. Kirk, E. Lee, B. Redding, M. Rosiek, D. Soltesz, B. Sucharski, T. Sucharski, and J. Torson (project engineer). The Ames MER team and M. Lemmon developed software to merge focal sections and generate anaglyphs from them. The MER Rover Planners provided excellent support of the MI investigation by commanding the instrument arm and MI dust cover. Reviews of this manuscript by J. Bishop, M. Chapman, J. Kargel, and an anonymous referee are much appreciated. This research was carried out for the Jet Propulsion Laboratory, California Institute of Technology, under a contract with the National Aeronautics and Space Administration.

Plates Referenced in Article

www.sciencemag.org/cgi/content/full/306/5702/1727/DC1
Plates 6 to 10

15 September 2004; accepted 9 November 2004

REPORT

Localization and Physical Property Experiments Conducted by Opportunity at Meridiani Planum

R. E. Arvidson,[1]* R. C. Anderson,[2] P. Bartlett,[3] J. F. Bell III,[4] P. R. Christensen,[5] P. Chu,[3] K. Davis,[3] B. L. Ehlmann,[1] M. P. Golombek,[2] S. Gorevan,[3] E. A. Guinness,[1] A. F. C. Haldemann,[2] K. E. Herkenhoff,[6] G. Landis,[7] R. Li,[8] R. Lindemann,[2] D. W. Ming,[9] T. Myrick,[3] T. Parker,[2] L. Richter,[10] F. P. Seelos IV,[1] L. A. Soderblom,[6] S. W. Squyres,[4] R. J. Sullivan,[4] J. Wilson[3]

The location of the Opportunity landing site was determined to better than 10-m absolute accuracy from analyses of radio tracking data. We determined Rover locations during traverses with an error as small as several centimeters using engineering telemetry and overlapping images. Topographic profiles generated from rover data show that the plains are very smooth from meter- to centimeter-length scales, consistent with analyses of orbital observations. Solar cell output decreased because of the deposition of airborne dust on the panels. The lack of dust-covered surfaces on Meridiani Planum indicates that high velocity winds must remove this material on a continuing basis. The low mechanical strength of the evaporitic rocks as determined from grinding experiments, and the abundance of coarse-grained surface particles argue for differential erosion of Meridiani Planum.

The Mars Exploration Rover (MER) Mission required accurate tracking of the location of Opportunity to ensure efficient drives and to place measurements in proper geological context, e.g., associating a rock target with a particular terrain or geologic unit (*1*–*3*). The location of the lander in inertial coordinates was determined by fitting direct-to-Earth, two-way, X-band Doppler radio transmissions and two passes of two-way Ultra High Frequency (UHF) Doppler transmissions between Opportunity and the Mars Odyssey Orbiter. Based on analyses of these observations, the landed location is 1.9483°S (with an accuracy of ~10 m) and 354.47417°E (with an accuracy of ~10 cm), translated to International Astronomical Union (IAU) 2000 areocentric coordinates. The landed location was also tied to Mars Global Surveyor (MGS) Mars Orbital Camera and MER descent image data to within ~10-m accuracy, by triangulation to three craters observed in the far field [through breaks in the local Eagle crater rim (*4*)] in Pancam images. These triangulation results, mapped to the cartographic network–derived MGS Mars Orbital Laser (MOLA) data (*5*), imply that the lander is located at 1.9462°S, 354.4734°E in IAU 2000 areocentric coordinates.

Opportunity stopped on the plains for a software upload on sols 75 to 78 (*6*), and its location (1.94752°S, 354.47716°E) was determined by analysis of two passes of UHF two-way Doppler tracking. The location was also determined by image-based triangulation to common features, with resultant values of 1.9453°S, 354.4766°E. For both landing and software-upload locations, the Doppler-based location was displaced 135 m

at an azimuth of 176° clockwise from north from the location derived from image-based analyses. This displacement is consistent with expected offset errors between inertially derived locations and positions estimated from the MOLA-based global cartographic network (*5*). These offsets provide a quantitative description of map errors expected for Mars in the equatorial regions when the current cartographic framework is used.

The first 57 sols of operations were conducted within Eagle crater (*6*), taking advantage of extensive rock outcrops exposed on the northwestern side of the crater. Slopes from the crater floor to the outcrops ranged up to 20° from horizontal and were covered by soils (*7*). The soil-covered slopes caused wheel slip and forced the MER team to plan novel approaches to rock targets. To traverse from one portion of the outcrop to another, Opportunity traveled across the crater floor and then turned directly upslope to approach a given rock target. In some cases, the rover used visual odometry to update positional information by acquiring stereo image data during traverses and using the range information to update positional knowledge. Observed slippage during upslope traverses of soil slopes of <10° was <20% in all cases, with more slip encountered at higher slopes. For example, 100% slip was encountered during the vehicle's initial attempt on sol 56 to egress from the crater on soil-covered slopes tilted at ~17°. The rover successfully completed egress on sol 57 by traversing at an oblique angle to the crater wall's topographic contours. These slip values are similar to those found during experiments in which the MER test rover traversed over dry, loose, poorly sorted, sand-sized materials.

For localization in Cartesian coordinates, we used forward- and backward-looking overlapping images of the surface, images of the sun, on-board inertial measurement unit (IMU) observations of rover tilt vectors, and tracking wheel turns in a least squares bundle-adjustment procedure to derive detailed positional estimates (Fig. 1). The magnitude of wheel slip within Eagle crater is evident, in that use of the bundle-adjustment technique and comparisons to positional estimates based on wheel turns alone demonstrate an accumulated error of 20 m over a total traverse distance of 183 m. For typical traverses of several meters, the rover position was delineated with an accuracy of several centimeters with the bundle-adjustment techniques.

Measurements of suspension system angles, together with rover tilt as inferred from IMU data, were used to reconstruct the elevation of each wheel at a 2- to 8-Hz sampling rate, relative to the start of each traverse (Fig. 1). Profile data retrieved for the sol 82 traverse across the plains show a height standard deviation of only 3.2 cm over the first 55 m and 40.3 cm over the total traverse distance of 141 m. These values are comparable to the small height standard deviations (<2 m over a 75-m-long scale) derived from pulse spreading observed in MOLA data (*8*), confirming the very smooth and flat nature of Meridiani Planum and the landing site. The smooth nature of the plains is occasionally interrupted by troughs and hollows that are typically several meters across or narrower, with depths less than several tens of centimeters (Fig. 1). Low-amplitude ripples (only several centimeters high) with wavelengths of less than a meter are ubiquitous on the plains.

Dust accumulation at the Meridiani Planum landing site is evident from analyses of Pancam data that show gradual reddening over 90 sols of the Pancam calibration target

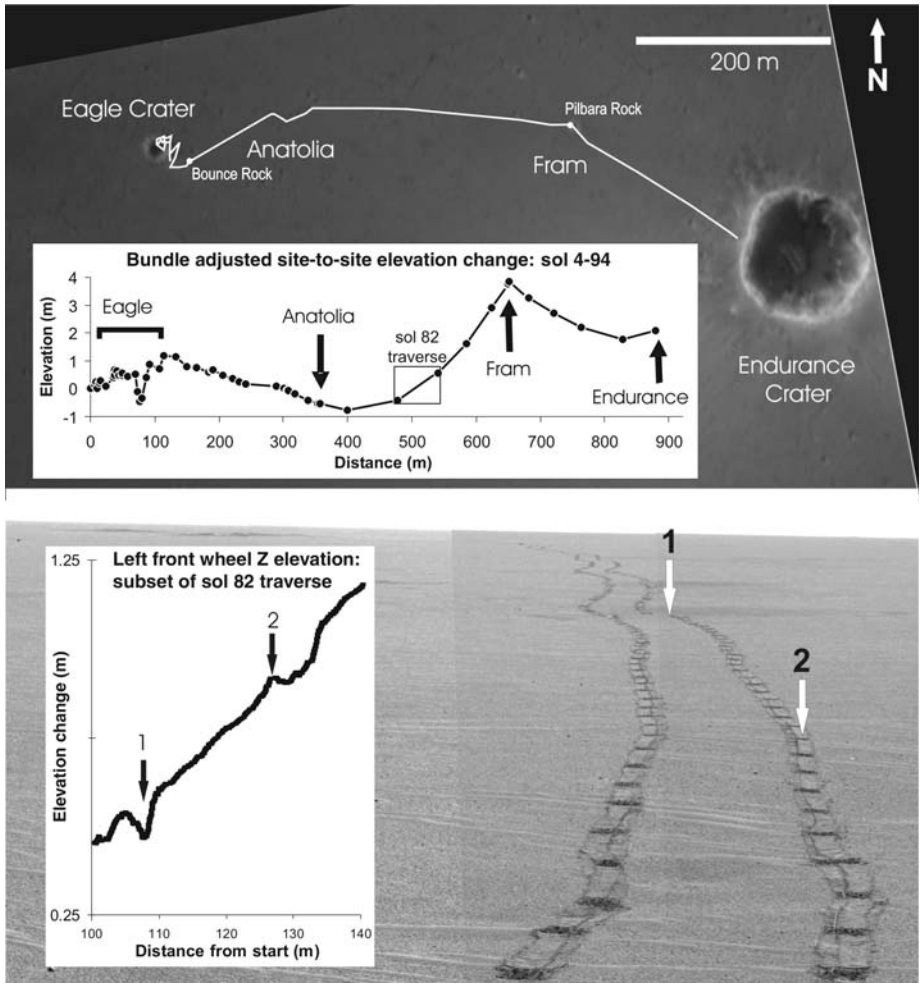

Fig. 1. (**Top**) MER Descent Image Motion Estimation System image showing traverses from the Eagle to Endurance craters, with stops at the Anatolia trough and Fram crater (image no. 1E128278513EDN0000F0006N0M1). (**Inset**) An elevation profile extracted from bundle-adjustments along the traverses. The dots on the profile correspond to localization stations for which backward- and forward-looking images were acquired. The relatively high elevation at the Fram location is interpreted to be due to a regional-scale but gentle rise and not due to the presence of the crater. The locations of the Bounce rock and Pilbara rock targets for the RAT are also shown. (**Bottom**) Pair of Pancam sol 82 images and vertical topographic profiles for traverses retrieved from rover tilt and wheel suspension data (Pancam frame nos. 1P135559477EFF1200P2431L7M1 and 1P135559499EFF1200P2431L7M1). Dark marks on the wheel tracks are associated with tie-down wheel cleats and are ~80 cm apart. Two shallow troughs are delineated by arrows at positions 1 and 2, and the low-amplitude ripples are evident in the foreground.

[1]Department of Earth and Planetary Sciences, Washington University, St. Louis, MO 63130, USA. [2]Jet Propulsion Laboratory, California Institute of Technology, Pasadena, CA 91109, USA. [3]Honeybee Robotics, 204 Elizabeth Street, New York, NY 10012, USA. [4]Department of Astronomy, Space Sciences Building, Cornell University, Ithaca, NY 14853, USA. [5]Department of Geological Sciences, Arizona State University, Tempe, AZ 85287, USA. [6]U.S. Geological Survey, Flagstaff, AZ 86001, USA. [7]NASA Glenn Research Center, Cleveland, OH 44135, USA. [8]Department of Civil and Environmental Engineering and Geodetic Science, The Ohio State University, Columbus, OH 43210, USA. [9]NASA Johnson Space Center, Houston, TX 77058, USA. [10]Deutsches Zentrum für Luft und Raumfahrt, Institut für Raumsimulation, Linder Höhe, Köln, D-51170, Germany.

*To whom correspondence should be addressed. E-mail: arvidson@wunder.wustl.edu

(*9*). Furthermore, analyses of short-circuit current-monitor solar cell data show a decrease in current of 0.29% per sol (corrected for seasonal variations in the Mars-sun distance and solar elevation angle) during the first 25 sols of operations, slowing to 0.13% per sol by sol 90. These values are comparable to those seen by Spirit at Gusev crater (*10*). Yet the MGS Thermal Emission Spectrometer–based bolometric albedo at the Meridiani site is only ~0.15 (*11*), consistent with Opportunity's observations that show that dust is a minor surface component in Eagle crater and on the plains (*9*, *12*). High-velocity winds must periodically scour the surface and remove surface dust accumulations from Meridiani Planum on a frequent basis.

The soils exposed at the Meridiani Planum landing site are dominated by dark, sand-sized and finer grained (<0.125 μm) basaltic materials overlain by sparsely to densely arrayed spherules and irregular particles with grain sizes that range up to a few millimeters across (*13*). Trenches excavated to 8- to 10-cm depths in soils on sols 23, 54 (both in Eagle crater), and 73 [adjacent to the Anatolia trough (Fig. 1)] show that these coarser grains are also found within the soils but at lower concentrations than on the surface (*14*). The spherules have a hematitic signature and have been found in outcrops observed by the rover (*9*, *12*, *15*, *16*). The high concentration of spherules and irregular particles at the surface is interpreted to be due to differential aeolian erosion of the evaporitic sedimentary rocks found by Opportunity (*16*), leaving behind a lag or pavement of relatively large and thus immobile materials. In addition, coarse-grained sand deposits have been reworked by wind to cover the ripples that are ubiquitous on the plains. The cores of the ripples are dominated by sand-sized and finer grained basaltic materials (*13*) (Fig. 2).

The physical nature of the soils within Eagle crater and on the plains can be inferred from a number of lines of evidence. Examination of wheel tracks shows that these deposits form high-fidelity casts of outer wheel surfaces, including cleat impressions with slopes greater than the angles of repose expected for most cohesionless materials. Impressions made by the Mössbauer contact plate (switch-activated when 1-N force was applied to soil surfaces) (Fig. 2), together with airbag bounce marks, show that spherules and irregular particles have been pressed into and partially covered by the finer grained soils (*13*), indicating that the uppermost fine-grained particles are easily displaced. In other cases, the spherules and irregular particles pressed into soils displace and expose millimeter-thick surface crusts. Furthermore, airbag seams are preserved well in bounce marks, and drag marks show complex curvilinear shapes with little indication of surface crumbling. All of these observations suggest that soils are only weakly cohesive (cohesive strength, ~1 to 3 kPa) and consist of sand-sized and smaller grain sizes, allowing the fine-grained component to fill voids between the larger grains during remolding of the soils.

With regard to standard soil mechanical properties, the estimated bearing strength of the Eagle crater floor soils, based on wheel track sinkage values (*17*) and on the depth of depressions made by the Mössbauer contact plate, average ~80 kPa with ~5 kPa of cohesive strength and an angle of internal friction of ~20°. The soils on the crater walls adjacent to the outcrops have an estimated bearing strength of ~8 kPa cohesion of ~0.5 kPa, and an angle of internal friction of ~20°. Motor currents associated with soil trenching operations show that soils are more easily excavated at Meridiani Planum, as opposed to the Spirit landing site in Gusev crater (*10*), and that excavation into a ripple on the floor of Eagle crater required the least amount of trenching energy. This result suggests that the soil deposits on the floor of the crater were modified relatively recently by winds and have not yet had the time to become cohesive.

Rock outcrops within Eagle crater ground by the Rock Abrasion Tool (RAT) (*18*, *19*) are of sedimentary origins (*13*) and include McKittrick (sol 30), Guadalupe (sol 34), and Flatrock (sol 44). Pilbara, another sedimentary rock located on the rim of Fram crater (Fig. 1), was ground on sol 86. Bounce rock, an igneous rock located on the plains near Eagle crater (Fig. 1), was ground on sol 66. Grinding of the McKittrick outcrop is illustrative of the multicomponent nature of the rocks exposed in Meridiani Planum. Two spherules were

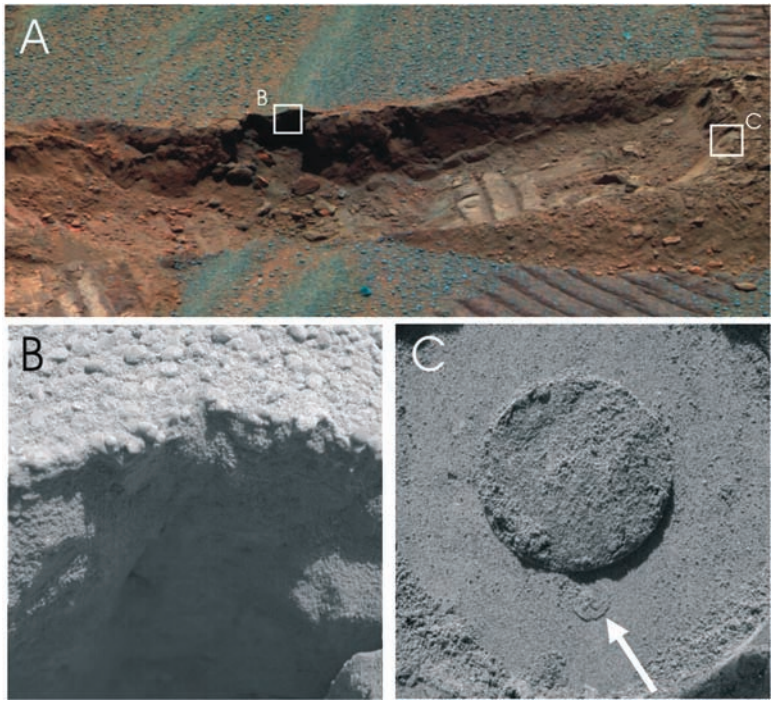

Fig. 2. (**A**) Pancam color mosaic of the Dog Track trench (image no. 1PP081EFF10CYL-CIP2421L256C1_full) excavated into soils at the Anatolia trough and acquired on sol 80. The trench is 8 to 10 cm deep. Boxes B and C show the locations of the Microscopic Imager (MI) images shown in (**B**) and (**C**). (**B**) MI frame (no. 1M135284929EFF10CGP2956M2M1) showing a monolayer or pavement of coarse sand on a ripple surface whose volume is dominated by sand and finer grained soils. (**C**) MI frame (no. 1M135284013EFF10CGP2956M2M1) showing the Mössbauer faceplate impression in soil, including the well-defined cast of a screw head on the faceplate.

Table 1. Rock energy/volume for RAT grinding for targets for the Gusev crater and Meridiani Planum (bold text) sites and selected rocks ground in the laboratory. Descriptions of terrestrial rock samples and targets ground by the Spirit rover at the Gusev site are given in (*10*). The table provides updated values for the Spirit rocks. Opportunity rock values are from (*19*).

Rock target	Grindability (J/mm³)
Terrestrial non-vesicular basalt	66–133
Terrestrial dolomite	85
Gusev Humphrey rock	83
Gusev Mazatzal rock	65
Gusev Adirondack rock	51
Terrestrial limestone	17–21
Guadalupe	**7.3**
Terrestrial shale	5.2
Bounce rock	**3.7**
Pilbara	**1.0**
McKittrick	**0.92**
Flatrock	**0.45**

encountered during grinding, and their high grinding resistance relative to the weaker rock matrix caused the RAT to stop operations (Plate 8). One spherule was slightly rotated during the grinding, and an irregular clast was plucked from the rock and thrown downhill during grinding. The estimated grinding energies for the rock targets at Meridiani Planum are relatively low, as compared to rocks at Gusev crater and most samples ground in the laboratory (Table 1). The grind energy correlates with the slope angles for the outcrop, in that the more resistant Guadalupe target ground by the RAT is located on a 36 ± 5° slope, whereas the less resistant McKittrick target is located on a 6.7 ± 2° slope. The higher slope for the Guadalupe outcrop is interpreted to be due to higher resistance to weathering than the McKittrick outcrop. Finally, even Bounce rock is weaker than rocks ground at Gusev crater, consistent with the densely fractured appearance of this rock (Plate 12). Bounce rock is an isolated target on the plains and was probably transported to its current location as impact ejecta (*12*). The fractures may have been introduced during ejection and impact of this rock.

The hematite-bearing plains that Opportunity landed on are at the top of a section of layered strata that is ~300 m thick and that disconformably overlies the Noachian-aged cratered terrain (*11*). We interpret the smooth, flat nature of Meridiani Planum to be due to differential stripping of horizontally layered strata, combined with continuing diffusion-driven mobilization of loose material to fill local depressions; i.e., soil fills in the craters, hollows, and troughs. Spherules, irregular particles, coarse sand covers, and basaltic soils represent the net result of concentration of these particles as the spherules were eroded from the weak evaporitic rocks in former and current aeolian environments. The hematite signature observed from orbit (*20*) that led us to land Opportunity in Meridiani Planum is due to a concentration of hematite-rich spherules that occurred as they were eroded from the evaporitic rocks. The lack of evaporite deposits in the soils on Meridiani Planum is due to relatively rapid aeolian erosion and removal as dust in suspension of these mechanically weak deposits. The amount of erosion is not well constrained, but it could range from meters to many meters.

References and Notes

1. S. W. Squyres *et al.*, *J. Geophys. Res.* **108**, 8062 (2003).
2. R. E. Arvidson *et al.*, *J. Geophys. Res.* **108**, 8070 (2003).
3. R. Li *et al.*, *J. Geophys. Res.* **107**, 8005 (2002).
4. Names have been assigned to areographic features by the Mars Exploration Rover (MER) Team for planning and operations purposes. The names are not formally recognized by the International Astronomical Union.
5. M. P. Golombek *et al.*, *J. Geophys. Res.* **108**, 8072 (2003).
6. A martian solar day has a mean period of 24 hours 39 min 35.244 s and is referred to as a sol to distinguish this from a roughly 3% shorter solar day on Earth.
7. The term martian soil is used here to denote any unconsolidated materials that can be distinguished from rocks, bedrock, or strongly cohesive sediment. No implication of the presence or absence of organic materials or living matter is intended.
8. G. A. Neumann *et al.*, *Geophys. Res. Lett.* **30**, 1561 (2003).
9. J. F. Bell III *et al.*, *Science* **306**, 1703 (2004).
10. R. E. Arvidson *et al.*, *Science* **305**, 5685 (2004).
11. R. E. Arvidson *et al.*, *J. Geophys. Res.* **108**, 8073 (2003).
12. P. R. Christensen *et al.*, *Science* **306**, 1733 (2004).
13. L. A. Soderblom *et al.*, *Science* **306**, 1723 (2004).
14. K. E. Herkenhoff *et al.*, *Science* **306**, 1727 (2004).
15. G. Klingelhöfer *et al.*, *Science* **306**, 1740 (2004).
16. S. W. Squyres *et al.*, *Science* **306**, 1698 (2004).
17. L. Richter, P. Hamacher, paper presented at the 13th Conference of the International Society for Terrain-Vehicle Systems, Munich, 14 to 19 September 1999.
18. S. P. Gorevan *et al.*, *J. Geophys. Res.* **108**, 8068 (2003).
19. T. M. Mynck *et al.*, paper 2004-6096 presented at the American Institute of Aeronautics and Astronautics (AIAA) Space 2004 Conference and Exhibit, San Diego, CA, 28 to 30 September 2004.
20. T. M. Christensen *et al.*, *J. Geophys. Res.* **105**, 9623 (2000).

21. We thank the MER Team and the scientists and engineers who made the landing, traverses, and science observations a reality. Work funded by NASA through the MER Project.

Plates Referenced in Article

www.sciencemag.org/cgi/content/full/306/5702/1727/DC1
Plates 8 and 12

18 August 2004; accepted 13 October 2004

RESEARCH ARTICLE

Mineralogy at Meridiani Planum from the Mini-TES Experiment on the Opportunity Rover

P. R. Christensen,[1]* M. B. Wyatt,[1] T. D. Glotch,[1] A. D. Rogers,[1] S. Anwar,[1] R. E. Arvidson,[2] J. L. Bandfield,[1] D. L. Blaney,[3] C. Budney,[3] W. M. Calvin,[4] A. Fallacaro,[4] R. L. Fergason,[1] N. Gorelick,[1] T. G. Graff,[1] V. E. Hamilton,[5] A. G. Hayes,[6] J. R. Johnson,[7] A. T. Knudson,[1] H. Y. McSween Jr.,[8] G. L. Mehall,[1] L. K. Mehall,[1] J. E. Moersch,[8] R. V. Morris,[9] M. D. Smith,[10] S. W. Squyres,[6] S. W. Ruff,[1] M. J. Wolff[11]

The Miniature Thermal Emission Spectrometer (Mini-TES) on Opportunity investigated the mineral abundances and compositions of outcrops, rocks, and soils at Meridiani Planum. Coarse crystalline hematite and olivine-rich basaltic sands were observed as predicted from orbital TES spectroscopy. Outcrops of aqueous origin are composed of 15 to 35% by volume magnesium and calcium sulfates [a high-silica component modeled as a combination of glass, feldspar, and sheet silicates (~20 to 30%)], and hematite; only minor jarosite is identified in Mini-TES spectra. Mini-TES spectra show only a hematite signature in the millimeter-sized spherules. Basaltic materials have more plagioclase than pyroxene, contain olivine, and are similar in inferred mineral composition to basalt mapped from orbit. Bounce rock is dominated by clinopyroxene and is close in inferred mineral composition to the basaltic martian meteorites. Bright wind streak material matches global dust. Waterlain rocks covered by unaltered basaltic sands suggest a change from an aqueous environment to one dominated by physical weathering.

The Mini-TES has provided remote measurements of mineral abundances and compositions, thermophysical properties, atmospheric temperature profiles, and atmospheric dust and ice opacities at the Opportunity rover landing site in Meridiani Planum. Mini-TES is a Michelson interferometer that collects infrared spectra from 5 to 29 μm (339 to 1997 cm^{-1}) at a spectral sampling of 10.0 cm^{-1} (*1*–*3*). Mini-TES observations of varying raster size and dwell lengths were acquired during rover operations within Eagle crater and during the traverse across the plains between Eagle and Endurance craters (*4*, *5*). Coregistered panoramic camera (Pancam) observations (*6*) provide context and additional multispectral visible and near-infrared observations. Reflected downwelling atmospheric radiance has been removed from all spectra presented here with the use of Mini-TES sky observations to directly measure the atmospheric radiance (*7*, *8*).

Mg and Ca sulfate–rich outcrops. Among the most exciting discoveries at Meridiani is the occurrence of bedrock with high